27 August 2021

Gaseous detectors: operating principles, applications and simulations

Yan Yan Chan Linying Zhan
Supervisor: Dr. Archana Sharma
CERN, CH-1211 Geneva, Switzerland

Keywords: Gaseous detectors, Drift tubes, CSC, MSGC, Microdot chambers, Micromegas, Micropattern, GEM, TPC, RPC, TGC, RICH, electron avalanche, Garfield++, Magboltz

Summary

Gaseous detectors have always played an important role in the field of high-energy particle physics. In this report, the operating principles of different types of gaseous detectors used in high-energy physics experiments are presented, followed by the application of gaseous detectors in various fields and the environmental issues of gaseous detectors operation. In addition, the programme Garfield++ that is commonly used for gaseous detectors simulation, is introduced. Lastly, a computer simulation of electron avalanche inside a GEM using Garfield++ is carried out to investigate the effect of gas composition and impurities on GEM performance.

Contents

1 Introduction

A gaseous detector is an instrument that is capable of detecting ionizing particles or radiation. The first gaseous detector is invented by Rutherford and Geiger for detecting α particles based on the Townsend effect. [18] The detector consisted of a anode wire, coaxial with a gas-filled cylindrical cathode. A potential difference is then maintained between the electrodes, resulting in an electric field that attracts the electrons produced in the gas to the anode. If the potential is large enough, electrons possess high kinetic energies after collision with the neutral gas molecules, which can eventually cause secondary ionisation. The electrons produced are then accelerated again, causing further ionization. This electron multiplication process takes the form of a cascade called Townsend avalanche. Since the multiplication yields a signal proportional to the primary charge, this device is named 'proportional counter'.

Later, other variations of gaseous detectors had been developed based on the applied voltage on the electrodes. There are mainly four modes of operation for a gaseous detector, namely the ionisation region, proportional region, limited proportional region, and the Geiger Müller region. In the ionisation region, the applied voltage is too low for the creation of secondary ions. The measured current does not vary much with the applied voltage. The advantage of ionisation chambers is that they have no dead time; thus, they are preferred for high radiation rates measurement. In the proportional region, the applied voltage is above the threshold for electron multiplication, and the current generated is proportional to the number of ion pairs created by the incident radiation. Hence, the energy of the incident particle can be inferred from the measured pulse amplitude. In the limited proportional region, the applied voltage is higher than that in the proportional region. Since free electrons have much higher mobility compared with positive ions, an almost motionless cloud of positive ions is created during the electron avalanche process. This ion cloud leads to distortion in the electric field, resulting in nonlinear electron multiplication. As for the Geiger Müller region, the applied voltage is sufficiently high that the entire gas volume is ionised, giving identical pulses regardless of the energy of incident radiation. Additionally, Geiger Müller counters have deadtime as long as 200 - 400 μs, rendering them undesirable for high rates measurement.

In the late 1960s, the increasing demand for high-energy physics (HEP) detectors prompted the development of larger area and faster particle detectors. In 1967, the revolutionary multi-wire proportional chamber (MWPC) was invented by CERN's Georges Charpak. [8] An MWPC uses arrays of wires as anodes, which run through a gas-filled chamber with parallel conductive plates as cathodes. MWPCs soon be adopted in many HEP experiments thanks to their excellent time and spatial resolution, continuous sensitivity and high rate capability. For this invention, Charpak was awarded the Nobel Prize for Physics in 1992. Initially, the position resolution of MWPCs is limited by the wire spacing, which is at least a few mm. To further enhance the spatial resolution, the idea of drift time is exploited, leading to the invention of drift chambers with position accuracy up to 300 - 400 μm. Later, other new types of gaseous detectors such as Ring Imaging Cherenkov (RICH) and Time Projection Chambers (TPC) were also invented in the late 1970s. In 1988, Anton Oed in the Institute Laue-Langevin developed a novel gaseous detector concept called micro-strip gas chamber (MSGC), which significantly improves both the multi-track resolution and the rate capability by at least one order of magnitude. [16] However, MSGCs are rather fragile and lack long-term reliability because of discharges induced by the high electric field. In light of this, an alternative detector called Gas Electron Multiplier is developed by Sauli in 1997. [20] GEMs have comparable performance with MSGCs, but with greater durability; thus, GEM-based detectors have numerous applications in HEP, medical diagnostics, and other fields (See Section 3). Thanks to the continuing demand for HEP experiments, the development of gaseous detectors has been in leaps and bounds and more sophisticated and accurate gaseous detectors are being invented constantly.

The rest of the report consists of four main sections. In section 2, the major types of gaseous detectors used in HEP experiments are reviewed. In section 3, we look into the application of gaseous detectors in HEP, astrophysics, medical and biology, plasma diagnosis and homeland security. In section 4, the environmental concerns associated with the use of gaseous detectors are evaluated. In section 5, we carry out computer simulation of GEM using Garfield++, verifying the effect of gas composition and impurities on GEM performance.

2 Different types of gaseous detectors

2.1 Multiwire Proportional Chamber (MWPC)

A multiwire proportional chamber (MWPC) uses anode wires to receive the electrons knocked out from the gas atoms when charged particles pass through. The registered electrons will then be turned into signals that provide position and time information about the incident particles.

2.1.1 Drift Tube (DT)

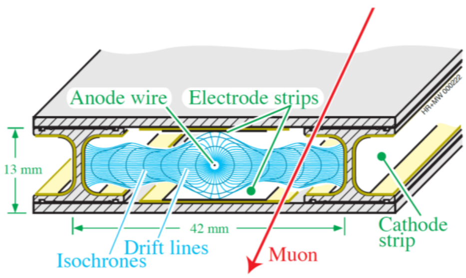

Figure 1: CMS drift tube

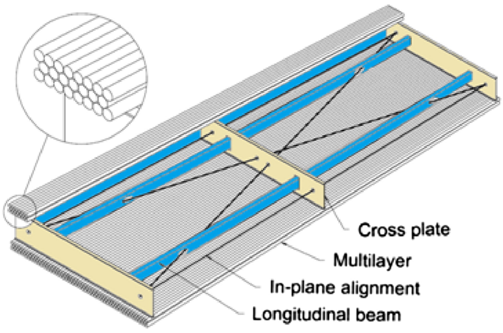

Figure 2: ATLAS drift chamber

A drift tube (DT) consists of an anode wire located at the center of a cathode tube filled with gases. Two coordinates, the incident particle's position along the wire and its distance away from the wire, are determined by measuring where the electrons hit on the wire, the electrons' drift time, and by using the space-time relationship. There are various ways to arrange a collection of drift tubes into a drift chamber, generally used for high precision muon tracking and momentum measurement, such as the one used in CMS muon system (Fig. 1 [23]). Meanwhile, the ATLAS muon system adopts a slightly different version, with the use of monitored drift tubes (MDTs) combined with an alignment system based on optical and temperature sensors (Fig. 2 [23]). [5] Some other derivatives include the Central Drift Chamber (CDC) used in the Belle-II experiment and the IDEA drift chamber (DCH) under design.

2.1.2 Cathode Strip Chamber (CSC)

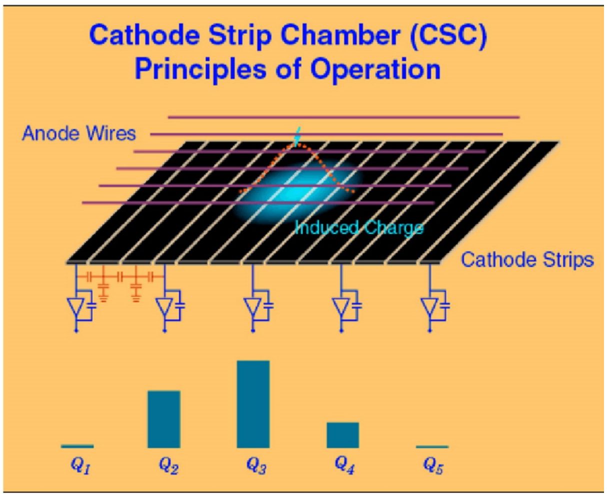

Figure 3: Working principles of Cathode Strip Chamber

Used in the CMS endcap region, Cathode Strip Chamber (CSC) is developed to withstand the uneven magnetic field and high particle rates. The perpendicularly arranged anode wires and cathode strips measure the two position coordinates of charged particles (Fig. 3 [23]). Its high space and time resolutions make it possible for both tracking and triggering. [23]

2.2 Micro-pattern Gas Detector (MPGD)

A micro-pattern gas detector (MPGD) uses microelectronic techniques to achieve high granularity with sub-millimeter distances between anode and cathode electrodes. It has several advantages compared to MWPC, such as excellent stability and radiation hardness, improved position and time resolutions, good energy resolution, ion backflow reduction, high rate capability and so on. [23]

2.2.1 Microstrip Gas Chamber (MSGC)

The main components of a microstrip gas chamber (MSGC) are an insulating or semi-insulating substrate engraved with closely spaced anode and cathode strips, and a metallized plane on top working as a drift electrode to define the drift field in the gas volume between (Fig. 4 [6]). Such geometry gives rise to the field lines shown in Fig. 5 [23] that allows the primary electrons created in the gas volume to drift towards the anode strips and produce Townsend avalanches. [9] The rate capability and gain are therefore increased.

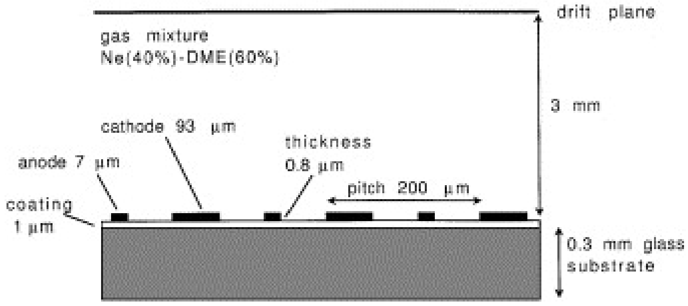

Figure 4: Schematics of CMS microstrip gas chamber (abandoned)

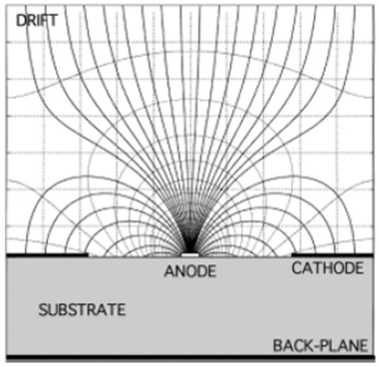

Figure 5: Electric field lines and equipotnetial lines of microstrip gas chamber

2.2.2 Microdot Chamber

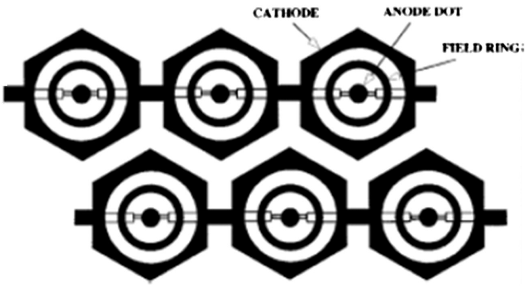

Figure 6: Schematics of microdot chamber

A microdot chamber is composed of a periodic structure of anode dots surrounded by cathode rings (Fig. 6 [23]). The change from strip-like geometry to dot-like geometry opens up the possibility for new gaseous pixel detectors. However, it has problems discharging despite its high gas gain [23] and good operational stability.

2.2.3 MICROMEGAS (MM)

A MICROMEGAS (MM) detector [10] is a parallel-plate chamber consisting of a cathode drift plane on the top, an anode microstrip plane at the bottom, and a drift region and a high field region separated by a layer of micromesh in the middle (Fig. 7 [23]). Electrons produced in the drift region enter the high field region and trigger avalanche due to the Townsend coefficient at high fields. Such an amplification allows for high gains, rates and stability with the minimum of ionizing particles. [23]

To improve the detector's efficiency at high rates, standard bulk MM is upgraded to the resistive MM to solve the problem of discharges induced dead time. Such a technique

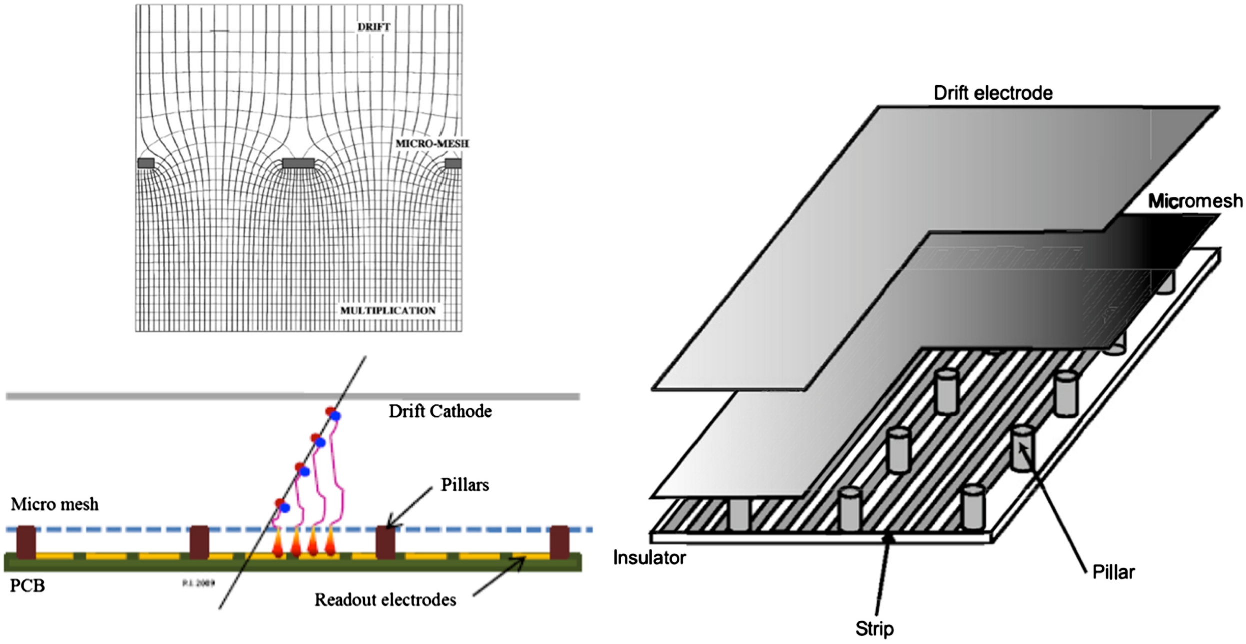

Figure 7: MICROMEGAS: (top left) electrical field, (bottom left) schematics, (right) electrode readout.

is applied in the ATLAS New Small Wheel (NSW) project to accommodate for the high luminosity (HL) upgrade of the Large Hadron Collider (LHC). As in Fig. 8 [14], a layer of resistive strips is added above the readout strips (separated by a layer of insulator) to suppress the intensity of discharge. [14]

In order to withstand even higher particle fluxes, the Resistive High granUlarity Micromegas project (RHUM) is underway to develop Resistive Pixelated MM aiming at high gain, high rate capability, high granularity and high stability. With the original readout strips replaced by small readout pads of only a few mm^2 area, the Resistive Pixelated MM achieves low occupancy under higher radiation, yet requires special resistive structure to optimize the discharge protection so as to avoid high-efficiency loss. [4] In Fig. 9 [4], two resistive schemes are displayed.

2.2.4 Gaseous Electron Multiplier (GEM)

As a hole-type gaseous detector, Gaseous Electron Multiplier (GEM) achieves electron amplification via a similar mechanism as MM with the high electric field induced in the hole of the copper-clad Kapton foil (Fig. 10 [23]). The possibility to use a cascade of GEM foils, or GEM together with other amplification devices like MSGC and MM, is its major advantage that promises high gains. In particular, triple GEM is the most commonly used version, providing high rate capability, high longevity, high stability, high spatial resolution and sufficient time resolution, making it suitable for muon tracking and triggering in high radiation environment. It is adopted in the LHCb muon system for triggering purpose and is the main character in the Phase 2 upgrade of the endcap region of the CMS muon system due to its above-mentioned advantage over traditionally used RPC. Among the three stations to

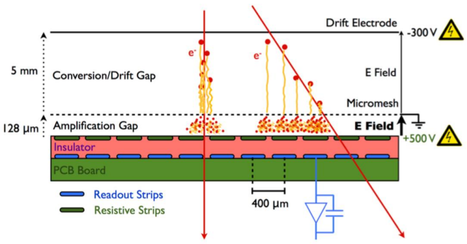

Figure 8: Schematics of MICRO-MEGAS layer in ATLAS NSW Project

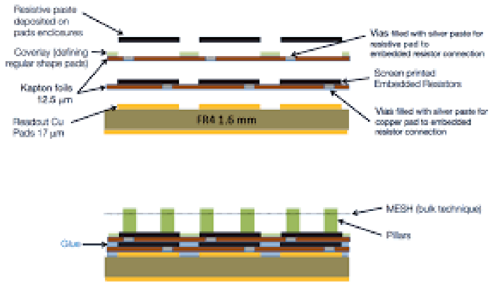

Figure 9: Resistive schemes of: (top) PAD-Patterned (PAD-P), (bottom) Diamond-Like Carbon (DLC)

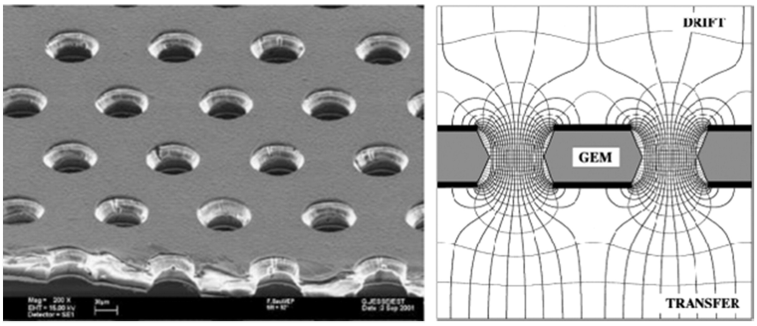

Figure 10: GEM: (Left) foil, (right) electric field and equipotential lines

be upgraded, GE1/1 and GE2/1 adopt double layers of triple-GEM chambers while ME0 employs six layers since it covers higher eta region with higher background (Fig. 11 [28]). Its application in these three stations is likely to prepare CMS for the HL-LHC. [28]

2.3 Other Gaseous Detectors

2.3.1 Time Projection Chamber (TPC)

The time projection chamber (TPC) is a large volume tracking apparatus, generally composed of a gas-filled cylindrical chamber with readout devices at the endcaps, as shown in Fig. 12 [23]. The cylindrical chamber is cut into halves by a central high voltage electrode which provides electric field along the length of the cylinder and often works under parallel magnetic field to minimize electron diffusion. Originally, TPC employs MWPCs as end plates for necessary signal amplification and readout, such as the one used in the ALICE 'central barrel' (Fig. 13 [3]). However, problems emerge concerning the space charge distortion in the drift region at high rates, which can be solved by replacing the MWPCs with MPGDs that has smaller ion backflow (IBF) from the amplification region into the drift region. Extensive researches in this area show that quadrupole GEM provides sufficient ion backflow suppression and good energy resolution, which is suggested for the upgrade of ALICE TPC. [1]

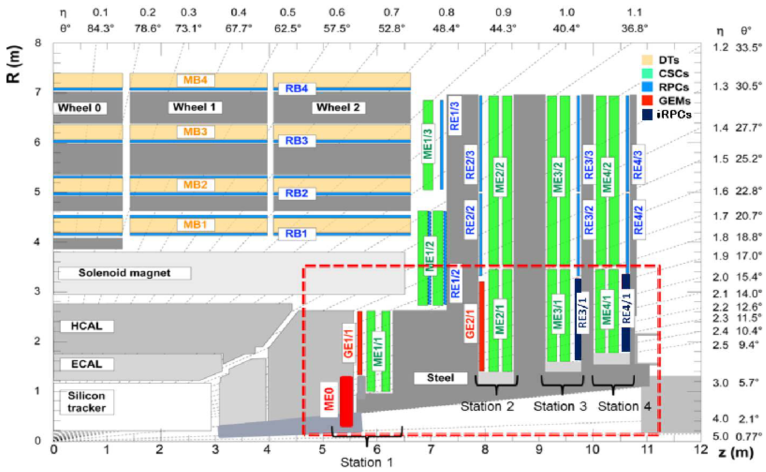

Figure 11: A quadrant of the CMS muon system

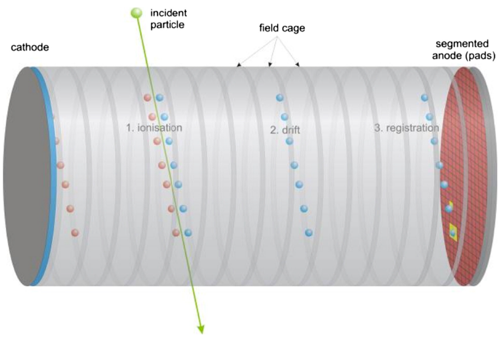

Figure 12: Schematics of time projection chamber

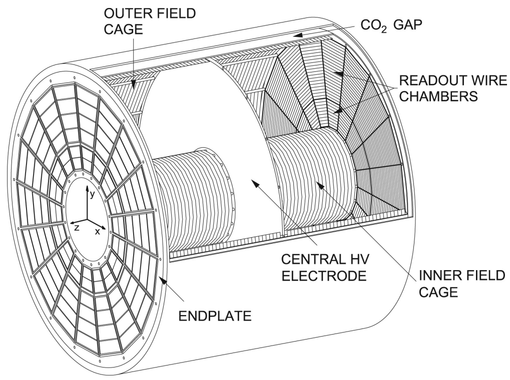

Figure 13: Schematics of ALICE time projection chamber

2.3.2 Resistive Plate Chamber (RPC)

A resistive plate chamber (RPC) consists of two parallel-plate graphite-painted electrodes of high resistivity with a small gas gap in between and some metallic read-out strips attached to an insulating film outside the graphite coating (Fig. 14 [23]). By running it in avalanche mode where signal amplification at the front-end level is applied to allow for lower gain at the initial stage, it achieves high rate capability and a combination of good spatial and time resolution, thus being appropriate for particle triggering under the high rate and background at LHC. A single RPC can be easily modified to include more gaps to achieve better time resolution, like the double-gap RPC used in CMS (Fig. 15 [23]) and the multigap RPC (MRPC) used for the ALICE time-of-flight (TOF) system (Fig. 16 [23]).

2.3.3 Thin Gap Chamber (TGC)

A thin gap chamber (TGC) has a CSC-like structure with anode wires sandwiched between two layers of high resistivity. The characteristic of TGC is the use of a special gas n-pentane which provides high gain with little sparks and little wire deposits. This allows the device to be built at very small drift distance and very close wire spacing, resulting in a good

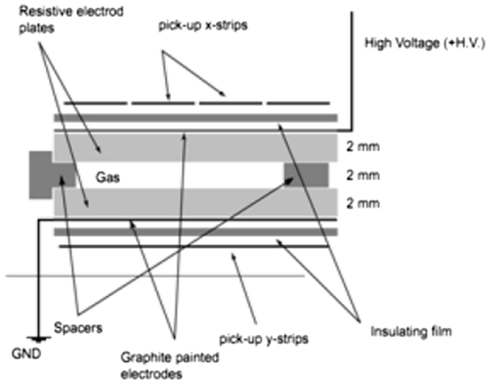

Figure 14: Schematics of single gap resistive plate chamber

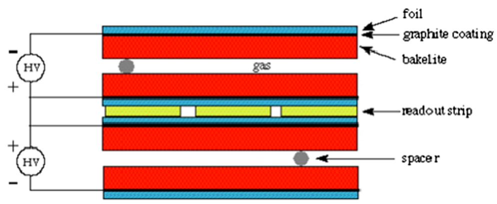

Figure 15: Schematics of double gap resistive plate chamber used in CMS

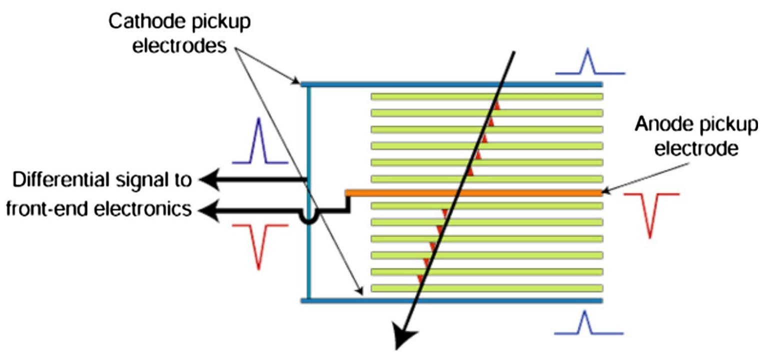

Figure 16: Schematics of multigap resistive plate chamber

time resolution suitable for muon triggering (Fig. 17 [23]). The consequent safety issues associated with its flammability need to be considered with great care. Meanwhile, Fig. 18 [2] shows a new technology called small-strip thin gap chamber (sTGC), which has smaller pitch between the readout strips compared to the original one. On each side of the anode plane, there are copper strips and pads behind the cathode planes as readout electrodes for coordinates measurement and triggering respectively. [2] It is applied in ATLAS NSW project to replace the old TGC used in its endcap muon spectrometer for fast triggering and high precision muon tracking under high rate environment. [2]

2.3.4 Ring Imaging Cherenkov (RICH)

A ring imaging Cherenkov (RICH) detector determines a charged particle's properties by measuring the Cherenkov radiation it emits when passing through a transparent refractive medium. In LHCb experiment, two RICH detectors are built to identify particles incoming at various speeds and angles.

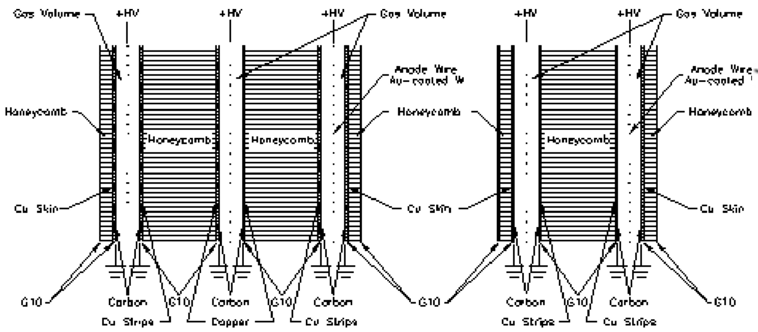

Figure 17: Schematics of thin gap chamber

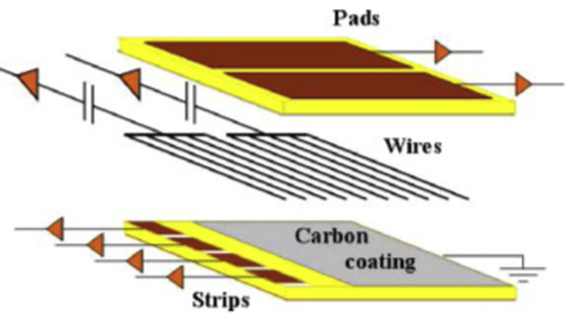

Figure 18: Schematics of small-strip thin gap chamber

3 Application of gaseous detectors

The ability of gaseous detectors in detecting ionizing particles enables a variety of applications, especially in particle physics, medicine and biology. In this section, we explore some of the most important applications of gaseous detectors in these areas.

3.1 High energy physics (HEP)

Gaseous detectors have been adopted extensively in HEP experiments for tracking and triggering of charged particles. In LHC, gaseous detectors are mainly used for muon tracking and triggering. For example, drift chambers, CSC, TGC, GEM, and resistive MM are used in CMS and ATLAS in the LHC for muon tracking and triggering. Whereas in ALICE, TPC is adopted for 3-dimensional tracking of muons. Outside LHC, TPCs are also used in other HEP experiments like the STAR detector at the Relativistic Heavy Ion Collidier (RHIC) and the inner tracker for Super Charm-Tau Factory for tracking of charged particles. Another application of gaseous detectors is to differentiate charged particles. For instance, RICH is used in LHCb for differentiating π/K and ALICE for differentiating π/K and p/K. Recently, MPGDs like GEM and MMs have been an active area of RD for their applications in future colliders due to their high radiation tolerance and outstanding resolution both spatially and temporally. [27]

3.2 Astrophysics

Applications of gaseous detectors in astrophysics can be classified into flight experiments, ground experiments, and underground experiments. For flight experiments, single-wire counters are used in satellite missions or balloon-borne missions to detect X-ray and gamma-ray signals that are otherwise undetectable on the ground. For example, two sets of proportional counters were adopted in the UHURU satellite mission launched in 1970, which led to the discovery of the pulsing accretion-powered binary X-ray sources. [15] Many ground-based experiments also use gaseous detectors for cosmic rays detection. For instance, RPCs are adopted in the Astrophysical Radiation Ground-based Observatory at YangBaJing (ARGO –YBJ) to reconstruct the space-time pictures of air showers front. Underground experiments are also essential in astrophysics for topics like neutrino physics, proton decay, and dark matter. The OPERA detector in the Gran Sasso Laboratory, one of the largest underground observatories, contains a magnetic muon spectrometer that makes use of RPCs.

3.3 Medicine and biology

Multi-wire proportional chambers are widely used in the medical field, such as digital radiography and angiography. [19] An X-ray scanner, which makes use of MWPCs, is developed by the Novosibirsk group and is used in low-dose medical examinations. Further development of this X-ray scanner leads to low-dose mammographic machines with the use of parallel-type MPGDs. One novel gaseous detector for radiotherapy is GEMPix, which is the combination of GEM and Medipix, a family of photon-counting pixel detectors. This new technology allows for 2D beam imaging in Intensity-Modulated Radiation Therapy (IMRT) with remarkable spatial resolution.

In biology, position-sensitive gaseous detectors play an important role in the imaging of beta-emitting radionuclides and macromolecular crystallography. MWPCs allow fast access to the intensity data and fast switching between frames, rendering them much preferable to photographic films for protein crystallography. [22] An innovative design of GEMPix, called GEMPix detector for microdosimetry with tissue-equivalent gas (GEMTEQ), is developed to study the temporal and spatial distributions of energy disposition on microscopic biological matters and retrieve information for microdosimetry. [13]

3.4 Plasma diagnosis

Gaseous detectors have been adopted in different areas of plasma diagnosis to examine plasma properties. For example, to investigate High-Frequency (HF) stationary plasma columns, pulsed discharges and arcs in the Kapitza Laboratory, MWPCs are used to measure the absorption of radiation of unknown spectral density, and hence reconstruct the soft X-ray spectrum from attenuation measurements. [12] The growing popularity of MPGDs also leads to the application of GEMs on plasma imaging. An innovative device based on a pinhole camera coupled with a GEM equipped with a 2D micropixel readout plate is developed for x-ray imaging of the plasma at a rate up to 100 kHz in a selectable x-ray energy range. [17] This technology is essential for the Tokamak fusion experiment to study the evolution of plasma and 2D-imaging during magnetohydrodynamics activities.

3.5 Homeland security

Besides research purposes, gaseous detectors are also extensively adopted in security scanning, such as inspection of cargo and individuals at airports. One way to inspect dense cargoes is muon tomography, which gives information about the inspecting objects based on the measurement of multiple Coulomb scattering of muon across the volume. For example, denser materials like leads and tungsten deflect muons more significantly than less dense materials like aluminum and plastics. [15] The muon tracking can be achieved by different large-area gaseous detectors like MWPC, DT, RPC and MPGD. Another type of common security scanning is using Radiation Portal Monitors (RPMs), which are passive radiation detectors used for the screening of individuals, vehicles and cargo for detection of traces of radiation at secure facilities. Currently, most RPMs are based on thermal neutron imaging using He-3 proportional tubes. These detectors measure the spontaneous emission of fast neutron emissions from special nuclear material, thus preventing the illicit trafficking of them.

4 Environmental issues of gaseous detectors

The performance of a gaseous detector depends largely on the choice of the gas mixtures used, which is a field under substantial research. Working under the high radiation environment, the gas mixtures need to satisfy the requirements of high drift velocity, large primary ionization yield (for tracking device), no secondary effects and fast ion mobility. [23] The most commonly used is a noble gas plus a quench gas, with the noble gas ensuring gas gain and the quench gas eliminating secondary effects. Polyatomic molecular and organic gas is a typical choice of quench gases since they can dissipate energy via molecular vibration and rotation, thus preventing secondary effects such as photon feedback and field emission. Among them, chlorofluorocarbons (known as freons) stand out due to their high stability and robustness at high rates. A great number of gaseous detectors, ranging from MPGD, TPC, RPC to RICH detectors, apply freons-based gases in their operation. This leads to concerns about their environmental impacts and future market under the F-gas regulation. [25]

Measures to reduce greenhouse gas (GHG) emissions include gas recirculation (system upgraded for ALICE TPC), gas recuperation (applied in CMS CSC, LHCb RICH-2, and understudy for RPC), leakage prevention (for present and future large volume gaseous detectors), and usage of green alternatives. [25] Efforts are made not only on the search for eco-gases compatible with the structures of the existing detectors but also on the construction of new detectors based on the use of eco-friendly gas mixtures. One of the major challenges of using eco-gas mixtures is their instability during the ionization process, which creates impurity that accelerates the aging of the detectors. Without considering this problem, a potential candidate for such transformation is the HFO-based gas mixture, which has smaller global warming potential (GWP) compared to that of freons. Its applications in RPC and CSC have been studied, producing promising results along with difficulties to be solved. In the case of the RICH detector, a new silicon photomultiplier (PM) improves the performance and so allows for CO_2 (in LHCb-RICH2) and C_4H_{10} (in LHCb-RICH1) to replace the use of freons. [24]

5 Simulation of electron avanlanche inside GEMs with Garfield++

Computer simulation of the performance of gaseous detectors is of paramount importance for design optimization and study of the electrostatic properties of various gaseous detectors. Currently, the most predominant programme for this purpose is Garfield++. In this section, we are going to use Garfield++ to simulate one of the most important types of gaseous detectors used at the LHC – GEM. The relevant simulation tools will first be briefly introduced, then the effect of gas mixture composition and gas impurities on the electron multiplication inside a GEM are examined with Garfield++.

5.1 Simulation tools

Garfield++ is an object-oriented tool that provides a detailed 3D simulation of particle detectors based on ionisation measurement in gases. [21] To calculate the gas transport properties, the Magboltz programme developed by Biagi [7] is integrated in Garfield++. And the ionization pattern produced along the track of relativistic charged particles is simulated by the Heed programme developed by Smirnov. [26] For 2D geometries consisting of wires, planes and tubes, a semi-analytic calculation based on the capacitance matrix method is implemented to obtain the field lines inside the gaseous detector. For 3D geometries, there is often no analytical solution and hence field maps are instead calculated using finite element programmes such as Ansys, Elmer, or COMSOL Multiphysics. The drift of charge carriers under an external E-field and B-field is calculated by Runge-Kutta-Fehlberg integration or Monte Carlo integration in Garfield++. [21]

5.2 Simulation parameters of GEM

In this paper, we simulate the drift of electrons and ions inside a standard GEM based on the example code in Garfield++. [21] The GEM consists of a 50 µm thick Kapton foil clad on both sides with a 5 µm layer of Copper. The holes where electron multiplication takes place are arranged in a hexagonal pattern, with an outer hole diameter of 70 µm, inner hole diameter of 50 µm, and pitch of 140 µm. The electric field inside the GEM is calculated with the finite element method with Ansys. The gas mixture used is Ar and CO_2. The effect of Ar/CO_2 ratios on GEM performance is examined in the next section. Since some of the excitation states of Argon possess excitation energy exceeding the ionisation energy of CO_2, i.e. 13.78 eV. These excited states can contribute to the gain by transferring energy to a CO_2 molecule through collisions or photo-ionisation. This is called the Penning effect, which is quantified by the probability r that excitation is converted to an ionising collision. The electron avalanches are simulated with a microscopic Monte Carlo method based on the electron-atom/molecule cross-section in the Magboltz database. Since ions cannot be tracked microscopically in Garfield++, the ion transport properties have to be provided from literature data.

The input parameters are summarised in Table. 1. The gas composition is not included in the table as they are the independent variables in this study.

5.3 Effect of Ar/CO_2 ratios on GEM Performance

Gas mixture composition plays an important role in GEM performance, and hence its long-term operation and stability. Hence, it is of paramount importance to study the effect of Ar/CO_2 ratios so as to optimize the performance of GEM. Conventionally, GEMs have a Ar/CO_2 ratio of 70/30, in which CO_2 is used as a quench gas to absorb photons produced from de-excitation as rotational or vibrational energies. As a result, the larger the proportion

Input parameter	values
Maximum energy of electron	200eV
Penning transfer probability r	0.57
Temperature	293.15K (room temp)
Pressure	760 Torr (1 atm)
Initial position of the electron	200 m above centre of the GEM hole
Initial energy of the electron	0.1 eV

Table 1: Table to input parameters of GEM simulation.

of CO_2, the less the electron avalanche is developed. Guida et al. have studied experimentally the effect of Ar/CO_2 ratios on the detector rate and gain of a GEM, showing that both decrease as the concentration of CO_2 increases. [11]

We verify the result from Guida et al. with Garifeld++ by investigating the plot of drift lines at different Ar/CO_2 ratios (Fig. 19). The results are consistent with our expectation as the smaller the portion of Ar in the mixture, the lower is the probability of primary ionization, leading to a lower amplification gain even if the ionization efficiency is high. Also, from Fig. 19a, we can see that there is an exceedingly significant electron multiplication in the absence of quench gas, resulting in spurious pulses and loss of proportionality. Therefore, it is critical to maintaining a stable gas composition inside GEMs.

5.4 Effect of gas impurities on GEM performance

In this section, we would like to investigate the effect of two different gas impurities, O_2 and N_2, on GEM performance. In the same paper by Guida et al., the effect of O_2 and N_2 as impurities on GEM performance have been examined since these are common gas impurities in the LHC gaseous detectors. [11] It is shown that the presence of 50 ppm (which is equivalent to 0.005%) oxygen decreases the detector rate gain by 20%, whereas 500 ppm (which is equivalent to 0.05%) of oxygen decreases the gain by 60%. Since O_2 has a high electron attachment coefficient, it tends to attract electrons produced in the avalanche, thus limiting the development of avalanche. Also, the decrease in rate suggests that the presence of O_2 also limits the primary ionisation inside the GEM. On the other hand, it is shown that N_2 concentration lower than 1% has little effect on the detector gain, whereas 5% of N_2 causes a significant 80% drop in the detector gain. Additionally, no specific effect on the detector rate is observed. This implies that N_2 is inert in the gas mixture, and the reduction in gain can be attributed to the reduced portion of Ar/CO_2 as the concentration of N_2 increases.

To investigate the effect of the presence of O_2 and N_2 using Garfield++, we keep the Ar/CO_2 ratio at a constant value of 7:3 and set the percentage of gas impurities to 1% and 10%. The simulation of electron avalanche is shown in Fig. 20. The case in which no impurity is present is shown in Fig. 20a as reference. The simulation results are in general in line with our expectation: the more the O_2 or N_2 present in the gas mixture, the fewer the number of electron/ion drift lines.

To conclude, computer simulation using Garfield++ is shown to be feasible to study the effect of gas mixture composition inside a GEM qualitatively. It is shown that the simulation

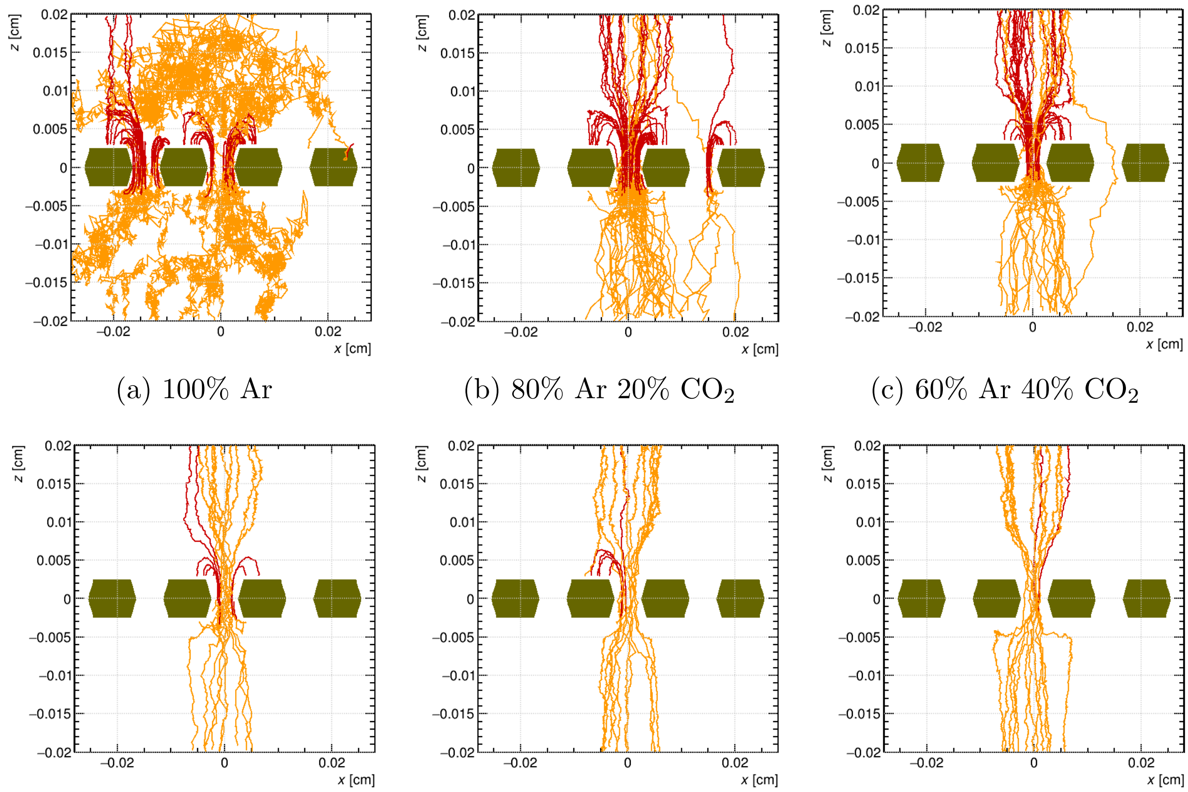

(a) 100% Ar

(b) 80% Ar 20% CO_2

(c) 60% Ar 40% CO_2

(d) 40% Ar 60% CO_2

(e) 20% Ar 80% CO_2

(f) 100% CO_2

Figure 19: Computer simulation of electron avalanche inside a GEM at different Ar/CO_2 ratios. Drifts of electrons are indicated by orange lines, whereas drifts of Ar or CO_2 ions are indicated by red lines.

results agree with that reported in Guida et al.'s paper, which can be summarised as below.

- Both detector rate and gain decreases as concentration of CO_2 increases
- Both detector rate and gain decreases at the presence of O_2 impurity
- GEM gain is stable when N_2 concentration is below 1%, and drop drastically for N_2 concentration greater than 5%

6 Conclusion

Gaseous detectors make use of the interaction between incident particles and gases, together with charge transfer and amplification technique, to study the identities and properties of ionizing particles. From multiwire proportional chambers (MWPCs) to micro-pattern gas detectors (MPGDs) to other gaseous detectors, different schematics provide distinct advantages and disadvantages suitable for detection in different circumstances. In light of the high-luminosity upgrade of LHC, efforts are made on new technologies such as MPGDs with resistive surfaces. Apart from high energy physics (HEP), gaseous detectors are widely applied in the fields of astrophysics, medicine and biology, plasma diagnosis and homeland

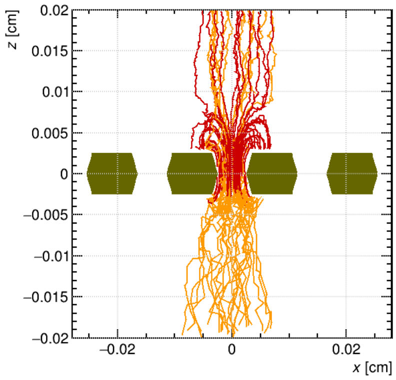

(a) 70% Ar 30%CO_2

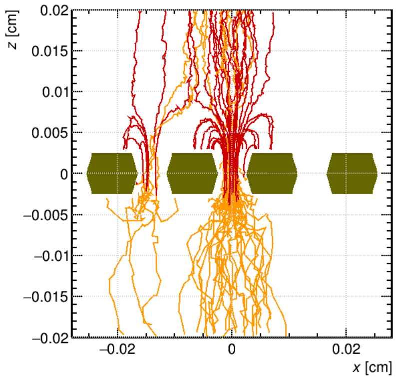

(b) 69.3% Ar 29.7% CO_2 1% O_2

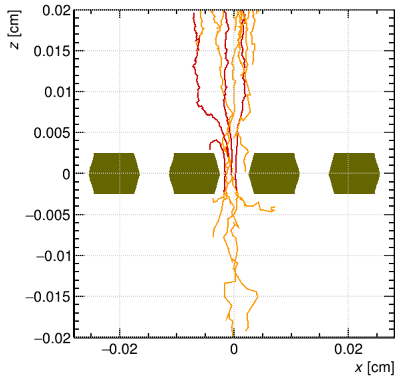

(c) 63% Ar 27% CO_2 10% O_2

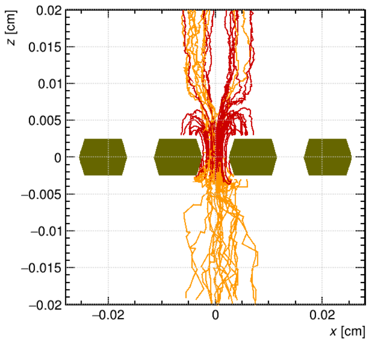

(d) 69.3% Ar 29.7% CO_2 1% N_2

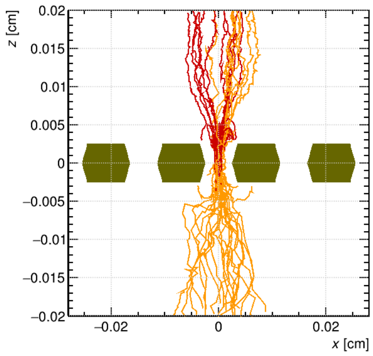

(e) 63% Ar 27% CO_2 10% N_2

Figure 20: Computer simulation of electron avalanche inside a GEM at the presence of gas impurities. Drifts of electrons are indicated by orange lines, whereas drifts of Ar or CO_2 ions are indicated by red lines.

security. However, since most gaseous detectors employed in HEP use freons as quench gases, it brings about environmental concerns that need to be solved by measures such as gas recirculation, gas recuperation, and the search of eco-gas alternatives. Lastly, we have simulated the electron avalanche inside a GEM with Garfield++, showing that the ratio of the gas mixture Ar/CO_2 affects the detector rate and gain of a GEM. While CO_2 serves as a necessary quench gas to achieve a balanced electron behavior, an increasing amount of it reduces the gas gain. Additionally, with a fixed Ar/CO_2 ratio, the presence of a certain amount of impurities with O_2 or N_2 also decreases the gas gain.

References

[1] Betty Abelev, J Adam, D Adamová, MM Aggarwal, G Aglieri Rinella, M Agnello, A Agostinelli, N Agrawal, Z Ahammed, N Ahmad, et al. Technical design report for the upgrade of the alice inner tracking system. *Journal of Physics G: Nuclear and Particle Physics*, 41(8):087002, 2014.

[2] Angel Abusleme, Camille Bélanger-Champagne, Alain Bellerive, Yan Benhammou, James Botte, Hadar Cohen, Merlin Davies, Yanyan Du, Lea Gauthier, Thomas Koffas, et al. Performance of a full-size small-strip thin gap chamber prototype for the atlas new small wheel muon upgrade. *Nuclear Instruments and Methods in Physics Research Section A: Accelerators, Spectrometers, Detectors and Associated Equipment*, 817:85–92, 2016.

[3] Johan Alme, Y Andres, H Appelshäuser, S Bablok, N Bialas, R Bolgen, U Bonnes, R Bramm, P Braun-Munzinger, R Campagnolo, et al. The alice tpc, a large 3-dimensional tracking device with fast readout for ultra-high multiplicity events. *Nuclear Instruments and Methods in Physics Research Section A: Accelerators, Spectrometers, Detectors and Associated Equipment*, 622(1):316–367, 2010.

[4] M Alviggi, V Canale, M Della Pietra, R De Oliveira, C Di Donato, E Farina, S Franchino, P Iengo, M Iodice, F Petrucci, et al. Construction and test of a small-pad resistive micromegas prototype. *Journal of Instrumentation*, 13(11):P11019, 2018.

[5] Christoph Amelung. The alignment system of the atlas muon spectrometer. *The European Physical Journal C-Particles and Fields*, 33(1):s999–s1001, 2004.

[6] R Bellazzini, M Bozzo, A Brez, A Cattai, G Gariano, L Latronico, R Loni, N Lumb, A Moggi, A Morelli, et al. The cms micro-strip gas chamber project–development of a high-resolution tracking detector for harsh radiation environments. *Nuclear Instruments and Methods in Physics Research Section A: Accelerators, Spectrometers, Detectors and Associated Equipment*, 457(1-2):22–42, 2001.

[7] SF Biagi. Monte carlo simulation of electron drift and diffusion in counting gases under the influence of electric and magnetic fields. *Nuclear Instruments and Methods in Physics Research Section A: Accelerators, Spectrometers, Detectors and Associated Equipment*, 421(1-2):234–240, 1999.

[8] Georges Charpak, R Bouclier, T Bressani, J Favier, and Č Zupančič. The use of multiwire proportional counters to select and localize charged particles. *Nuclear Instruments and Methods*, 62(3):262–268, 1968.

[9] Tom Francke and Vladimir Peskov. Micropattern gaseous detectors. In *Innovative Detectors for Supercolliders*, pages 158–179. World Scientific, 2004.

[10] Yannis Giomataris, Ph Rebourgeard, Jean Pierre Robert, and Georges Charpak. Micromegas: a high-granularity position-sensitive gaseous detector for high particle-flux environments. *Nuclear Instruments and Methods in Physics Research Section A: Accelerators, Spectrometers, Detectors and Associated Equipment*, 376(1):29–35, 1996.

[11] R Guida, B Mandelli, and M Corbetta. Effects of gas mixture quality on gem detectors operation. In *Journal of Physics: Conference Series*, volume 1498, page 012036. IOP Publishing, 2020.

[12] EL Kosarev, VD Peskov, and ER Podolyak. High resolution soft x-ray spectrum reconstruction by mwpc attenuation measurements. *Nuclear Instruments and Methods in Physics Research*, 208(1-3):637–645, 1983.

[13] Johannes Leidner, Fabrizio Murtas, Marco Silari, and Antonio Soave. Gemteq: Gempix detector for microdosimetry with tissue-equivalent gas.

[14] I Manthos, I Maniatis, I Maznas, M Tsopoulou, P Paschalias, T Koutsosimos, S Kompogiannis, Ch Petridou, SE Tzamarias, K Kordas, et al. The micromegas project for the atlas new small wheel. In *AIP Conference Proceedings*, volume 2075, page 080010. AIP Publishing LLC, 2019.

[15] Eugenio Nappi and Vladimir Peskov. *Imaging gaseous detectors and their applications*. John Wiley & Sons, 2013.

[16] A Oed. Position-sensitive detector with microstrip anode for electron multiplication with gases. *Nuclear Instruments and Methods in Physics Research Section A: Accelerators, Spectrometers, Detectors and Associated Equipment*, 263(2-3):351–359, 1988.

[17] D Pacella, G Pizzicaroli, M Leigheb, R Bellazzini, A Brez, M Finkenthal, D Stutman, B Blagojevic, R Vero, R Kaita, et al. Fast x-ray imaging of the national spherical tokamak experiment plasma with a micropattern gas detector based on gas electron multiplier amplifier. *Review of scientific instruments*, 74(3):2148–2151, 2003.

[18] Ernest Rutherford and Hans Geiger. An electrical method of counting the number of α-particles from radio-active substances. *Proceedings of the Royal Society of London. Series A, Containing Papers of a Mathematical and Physical Character*, 81(546):141–161, 1908.

[19] Fabio Sauli. Applications of gaseous detectors in astrophysics, medicine and biology. *Nuclear Instruments and Methods in Physics Research Section A: Accelerators, Spectrometers, Detectors and Associated Equipment*, 323(1-2):1–11, 1992.

[20] Fabio Sauli. Gem: A new concept for electron amplification in gas detectors. *Nuclear Instruments and Methods in Physics Research Section A: Accelerators, Spectrometers, Detectors and Associated Equipment*, 386(2-3):531–534, 1997.

[21] H. Schindler. Garfield++ user guide, version 2021.3, 2021.

[22] Georg E Schulz and Gerd Rosenbaum. The multi-wire proportional chamber as an area detector for protein crystallography in comparison with photographic film; guidelines for future development of area detectors. *Nuclear Instruments and Methods*, 152(1):205–208, 1978.

[23] Archana Sharma. Muon tracking and triggering with gaseous detectors and some applications. *Nuclear Instruments and Methods in Physics Research Section A: Accelerators, Spectrometers, Detectors and Associated Equipment*, 666:98–129, 2012.

[24] Archana Sharma. Designing gas transport parameters for future hep experiments, 21.06.2021.

[25] Archana Sharma. Greening gaseous detectors, 28.05.2021.

[26] IB Smirnov. Heed version 1.01. *Detailed Simulation of the Initial Ionization in Gases, CERN Computer Newsletter*, (226):13, 1996.

[27] Maxim Titov. New developments and future perspectives of gaseous detectors. *Nuclear Instruments and Methods in Physics Research Section A: Accelerators, Spectrometers, Detectors and Associated Equipment*, 581(1-2):25–37, 2007.

[28] Michael Tytgat et al. The triple-gem project for the phase 2 upgrade of the cms muon system. *PoS TIPP2014*, page 065, 2014.